Triosephosphate Isomerases in Italian Ryegrass (*Lolium multiflorum*): Characterization and Susceptibility to Herbicides

DANIELE DEL BUONO,*,[†] BHAKTI PRINSI,[§] LUCA ESPEN,[§] AND LUCIANO SCARPONI[†]

[†]Dipartimento di Scienze Agrarie e Ambientali, Università degli Studi di Perugia, Borgo XX Giugno 72, 06121 Perugia, Italy, and [§]Dipartimento di Produzione Vegetale, Università degli Studi di Milano, Via Celoria 2, 20133 Milan, Italy

The effect of treatments with four herbicides and a safener on the activity of triosephosphate isomerase (TPI) extracted from shoots of Italian ryegrass was investigated. It was found that atrazine and fluorodifen, herbicides which interfere with photosynthesis, caused a decrease in measured enzyme activity. In addition, the *in vitro* effect of oxidized glutathione (GSSG), a compound produced in situations of oxidative stress, on TPI activity was investigated. It was shown that GSSG was a strong inhibitor of enzyme activity, at low concentrations in a dose–time-dependent manner. The enzyme extracts were submitted to chromatographic purifications and to two-dimensional electrophoresis. Some spots had molecular masses ranging between 20 and 30 kDa and were characterized and identified by LC-ESI-MS/MS as TPIs. The mass spectrometry also made it possible to identify the presence of cysteine residues that could be subjected to *S*-glutathionylation, which regulate the enzyme activity.

INTRODUCTION

Triosephosphate isomerases (TPI, EC 5.3.1.1) are enzymes that catalyze the interconversion of dihydroxyacetone phosphate (DHAP) and D-glyceraldehyde 3-phosphate (GAP), and they are present in all living cells and tissues (*1, 2*). In detail, TPIs carry out an electrophilic catalysis in the enolization reaction, they show a higher affinity toward GAP than DHAP, and they possess a very high level of specificity toward the two substrates (*2–5*). TPIs are considered to be perfect catalysts, and they can be present in plants in plastidic isoform (pTPI), as a key enzyme in the Calvin cycle, or in cytosolic isoform (cTPI), which is involved in glycolysis and gluconeogenesis (*1, 4, 6*). By contrast, some green algae possess only chloroplast isoenzyme, and they lack the cytosolic isoform (*1, 7*). The level of TPI is strongly dependent on the age and stage of tissue development; in particular, it was found that the activity of cTPI was significantly higher in expanding leaves compared to mature senescing ones, because the growing leaves need energy and C skeletons from glycolysis and respiration for biosynthetic purposes (*2*). In addition, TPIs play a very important role in gluconeogenesis, fatty acid biosynthesis, pentosephosphate pathway (*8, 9*). Sequence analyses of several plastid genomes suggest that all of the enzymes of sugar phosphate metabolism in plastids are encoded from nuclear DNA and imported in the organelle with the aid of a transit peptide (*1*). The high degree of sequence conservation between plastidic and cytosolic TPIs suggests a low rate of evolutionary divergence, a feature common to all glycolytic enzymes (*9, 10*). Despite the importance of TPIs in metabolism, they have not been extensively

studied in plants, and in particular their response to stressing agents remains to be investigated in depth.

Some reports have shown how these enzymes are responsive to a variety of stressing agents: Deepika et al. (*11*) found different transcript levels of genes encoding glycolytic and fermentative enzymes, including TPI, induced by desiccation, salt, and high temperature. Umeda et al. (*12*) demonstrated how some ATP-generating enzymes, TPIs among them, were induced by saline and water stress conditions in rice cells; a coordinated induction of these enzymes for the production of energy to maintain the homeostasis in stressed cells was supposed. Also in maize, it was shown how water deficit increases the expression of some proteins comprising cTPI (*13*). Another study showed that, in a resistant genotype of *Brassica carenata*, TPIs and other enzymes of the Calvin cycle were significantly more induced upon pathogen infection than in a susceptible genotype (*14*). In the above cases, the induction of cTPI and pTPI provides supplementary energy and photosynthetic products to contrast these dangerous situations and permitting the plant's survival.

On the other hand, it was ascertained that a high cellular concentration of reactive oxygen species (ROS) can depress some metabolic pathways in which TPIs are involved (*15, 16*). It is well-known that ROS accumulation can result from abiotic and biotic stresses, and it acts by altering the redox status of the cells (*16–18*). This status is determined by the glutathione reduced (GSH)/glutathione oxidized (GSSG) ratio; in normal conditions the cells present a large amount of reduced glutathione, whereas an oxidative perturbation leads to an accumulation of oxidized glutathione (*19, 20*). High concentrations of GSSG bring about the *S*-glutathionylation of some proteins, which is the formation of a disulfide bond, via thiol–disulfide exchange reactions,

*Corresponding author (telephone +39 075 585 6225; fax +39 075 585 6239; e-mail delbuono@unipg.it).

between proteinaceous Cys and oxidized glutathione (*21*, *22*). When the cells return to a normal redox status, by recovering their physiological concentration of reduced glutathione, the proteins are deglutathionylated and then recover their activity (*21*). Following the above findings, S-glutathionylation is gaining attention for this protective and regulatory role for some proteins (*22*).

Herbicides are recognized among the chemicals causing oxidative perturbations in plants, and a large number of them cause oxidative stress. Some compounds, called herbicide safeners, are employed to protect crop plants against injury from certain herbicides, without reducing their action on the target weeds (*23*–*25*). Surprisingly, there are no literature reports on herbicide effects on TPIs, with the exception of a paper on the toxicity of paraquat on *Pisum sativum*, which shows a drop in the activity of the above enzymes (*26*). Therefore, one aim of this research was to ascertain the effect of some herbicides on TPI activity in Italian ryegrass (*Lolium multiflorum*), which was chosen as a model plant for its strong resistance to many herbicides (*27*, *28*). The herbicides atrazine, fluorodifen, metolachlor, and fenoxaprop-ethyl and the safener fenchlorazol-ethyl were employed because of their widespread use in weed control. Further aims were to determine if S-glutathionylation regulates the activity of the above enzymes and to increase knowledge on the TPIs of Italian ryegrass by their purification and characterization.

MATERIALS AND METHODS

Chemicals. Atrazine, fenchlorazol-ethyl, fenoxaprop-ethyl, fluorodifen, metolachlor, dihydroxyacetone phosphate, D-glyceraldehyde 3-phosphate, α-glycerophosphate dehydrogenase, NADH, and glutatione oxidized were supplied by Sigma Aldrich (St. Louis, MO). Urea, CHAPS, Pharmalyte, dithiothreitol, and iodoacetamide were supplied by GE Healthcare (Chalfont, U.K.). All other reagents were of ACS grade.

Plant Material and Growth Conditions. Italian ryegrass seeds (*L. multiflorum* 'Hellen') (40 g) were germinated in plastic flats (0.08 m^2) containing sand quartz prewashed with a solution of hydrochloric acid (10%, v/v) and sterilized with a solution of NaClO (5%, w/v). Seedlings were grown in the dark in a growth chamber at 18 °C (relative humidity = 80%). After 2 days, the seedlings were submitted to day/night conditions (12 h of light at 23 °C, light intensity 300 μmol m^{-2} s^{-1}, and 12 h of darkness at 21 °C) and watered daily. When the seedlings were 6 days old, the plants were divided into six groups: one group was left as the control, and the others were singly treated with atrazine (14.4 mg/flat), fenchlorazol-ethyl (4.43 mg/flat), fenoxaprop-ethyl (1.80 mg/flat), fluorodifen (14.4 mg/flat), and metolachlor (20.0 mg/flat) at the recommended field application rates. Shoots were collected at 48 h after the treatment, rinsed with water to remove nonadsorbed chemicals, dried by blotting with paper and subjected to the subsequent assays for TPI activity.

Each plant material preparation, plant extraction, enzyme assay, chromatographic purification and analytical determination was run in triplicate.

TPI Extraction from Plant Tissues and Assays of Enzyme Activity. The extraction of TPIs was carried out between 0 and 4 °C, and the enzyme assay was performed according to the method of Dorion et al. (*2*). In detail, shoots of Italian ryegrass (4.0 g) were ground to a fine powder in liquid nitrogen using a mortar and pestle. The powder was suspended in an extraction buffer (4/1, w/v) composed of 50 mM Tris-HCl (pH 8.0) containing 2 mM EDTA, 1 mM dithiothreitol, and 1.5% (w/v) polyvinylpolypyrrolidone. After filtration through two layers of muslin, the homogenate was centrifuged at 12000*g* for 20 min. The supernatant solution was then adjusted to 80% saturation with respect to (NH$_4$)$_2$SO$_4$ to precipitate the proteins (4 °C for 3 h). The resulting suspension was centrifuged at 12000*g* for 10 min and the protein pellet collected and stored at −20 °C. The pellet was dissolved in a buffer containing 20 mM Tris-HCl (pH 8.0) containing 1 mM dithiothreitol and applied onto a Sephadex G-25 column for desalting. The desalted proteins were used for enzyme activity assays. TPI was assayed in the GAP to DHAP direction in a coupled enzyme assay performed by adding 1 mM GAP to a solution containing 800 μL of 0.1 M Tris-HCl (pH 7.5), 0.5 mM EDTA, 0.5 U/mL

α-glycerophosphate dehydrogenase (α-GPDH, EC 11.1.8), 0.2 mM NADH, and 50 μL of enzyme extract. The TPI activity was determined by measuring the NADH disappearance at 340 nm. Blank reaction rate was also determined in the same mixture of the above assay without GAP; the enzyme activity was then subtracted from the rate determined in the nonenzymatic reaction. The specific TPI activity was expressed as nanomoles of GAP transformed per second per milligram of protein employed for the assay. Total protein concentration in the desalted protein extract was estimated by using the Bradford method (*29*).

Test of the Effect of GSSG on TPI Activity. TPIs of shoots of Italian ryegrass, extracted as described under TPI Extraction from Plant Tissues and Assays of Enzyme Activity, were incubated at 35 °C, over a time period of 7 h, in the absence or presence of different concentrations of GSSG. In detail, 2.05, 5.10, 10.20, 20.4, or 40.8 mM GSSG was added, and the specific enzyme activity was then monitored at 1, 3, 5, and 7 h after the start of incubation, as described in the previous paragraph.

Fast Protein Liquid Chromatography (FPLC) Purification. All purification steps were carried out between 0 and 4 °C to avoid protein degradation. Shoots of Italian ryegrass (30.0 g) were ground to a fine powder in liquid nitrogen using a mortar and a pestle. The powder was suspended in the extraction buffer, extracted, centrifuged, raised to 80% of saturation with (NH$_4$)$_2$SO$_4$, and desalted as described under TPI Extraction from Plant Tissues and Assays of Enzyme Activity. The desalted proteins were then applied to an anionic exchanger column (Q Sepharose FF column of 8 mL of volume; GE Healthcare), pre-equilibrated with 20 mM Tris-HCl (pH 7.5) containing 1 mM dithiothreitol. Initially the column was washed, at a flow rate of 4 mL min^{-1}, until the absorbance at 280 nm had returned to baseline. The column was then eluted, at a flow rate of 4 mL min^{-1} and collecting fractions of 4 mL, with the same buffer containing increasing concentrations of NaCl, from 0 to 0.5 M (total volume of 80 mL). Finally, the column was washed with 1 M NaCl (80 mL). To improve the purifications and isolate fractions adequate for two-dimensional SDS-PAGE analysis and mass spectrometry, the fractions showing TPI activity were recharged and chromatographed at a flow rate of 1 mL min^{-1}, collecting fractions of 1 mL by using increasing the concentration of NaCl from 0 to 0.5 M.

1D and 2D SDS-PAGE Analyses. Monodimensional SDS-PAGE analyses were performed according to the method of Laemmli (*30*). The proteins were suspended in the Laemmli buffer and denatured at 95 °C for 5 min. Each sample was submitted to 1D SDS-PAGE using a resolving gel containing 12.5% of acrylamide and a stacking gel containing 4% of acrylamide. The polypeptides were resolved under a constant current of 15 mA in an Amersham Hoefer miniVE Vertical Electrophoresis System. The gels were stained with colloidal Coomassie Brilliant Blue.

Two-dimensional SDS-PAGE analyses were performed according to the procedure of O'Farrel (*31*). Samples of proteins of Italian ryegrass shoots, extracted and purified as described above, were cleaned by precipitation, for 24 h at −20 °C, with TCA (20% in acetone) to remove interfering substances. The pellet was centrifuged, washed with acetone (80%), dried, and then dissolved in a buffer containing 8 M urea, CHAPS (0.5%, w/v), Pharmalyte (0.2%, v/v), and bromophenol blue (0.002%, w/v). IEF was performed on 7 cm long pH 4−7 Immobiline DryStrips at 200 V for 1 min, followed by a progressive increase from 200 to 3500 V for 90 min and a final constant step at 3500 V for 90 min. After IEF, the strips were briefly washed with water and saturated with an equilibration buffer consisting of 50 mM Tris-HCl (pH 8.8), containing 6 M urea, glycerol (30%, v/v), SDS (2%, w/v), and bromophenol blue (0.002%, w/v). Dithiothreitol and iodoacetamide were added to the strips buffer, in two subsequent steps, to preserve the fully reduced state of the proteins. The strips were placed on Excel Gel Homogeneous SDS 12.5% acrylamide, and analyses were performed using an Amersham Multiphor II at 120 V for 20 min followed by 70 min at 600 V. The gels were stained with colloidal Coomassie Brilliant Blue.

Protein In-Gel Digestion and LC-ESI-MS/MS Analysis. Spots excised from gels stained with colloidal Coomassie Brilliant Blue were digested as described by Magni et al. (*32*) with some refinements. In detail, after the destaining, the spots were dried under vacuum in a centrifugal evaporator and incubated in 10 mM dithiothreitol/100 mM NH$_4$HCO$_3$ for 45 min at 56 °C. The solution was replaced with 55 mM iodoacetamide/100 mM NH$_4$HCO$_3$, and the spots were incubated for 30 min in the dark at room temperature. After that, the spots were briefly washed with 100 mM

Table 1. 6-Day-Old Seedlings of Italian Ryegrass Were Singly Treated with Atrazine, Fenchlorazol-ethyl, Fenoxaprop-ethyl, Fluorodifen, and Metolachlor[a]

	specific TPI activity (nmol s^{-1} mg^{-1} of protein)
control	9.80 ± 0.43 a
atrazine	7.20 ± 0.21 b
fenchlorazol-ethyl	10.20 ± 0.41 a
fenoxaprop-ethyl	9.30 ± 0.50 a
fluorodifen	6.28 ± 0.17 c
metolachlor	9.57 ± 0.25 a

[a] The shoots were collected 48 h after treatment, and the desalted proteins were submitted to TPI activity determinations; the results were compared with those obtained for untreated shoots. The data represent the means of triplicate determinations. Means within the same column followed by the same letter are not significantly different at the 5% level using the *t* test.

NH$_4$HCO$_3$ and again incubated for 15 min in 50% (v/v) acetonitrile (ACN), for 3 min in ACN, for 3 min in 100 mM NH$_4$HCO$_3$, for 15 min in 50 mM NH$_4$HCO$_3$/50% (v/v) ACN, and finally dried under vacuum. The following stages, consisting of the protein digestion with trypsin (sequencing grade modified trypsin V5111, Promega, Madison) and the recovery of peptides, were carried out as described by Magni et al. (*32*).

The LC-ESI-MS/MS experiments were conducted using a Finnigan Surveyor (MS pump Plus) HPLC system directly connected to the ESI source of a Finnigan LCQ DECA XP MAX ion trap mass spectrometer (ThermoFisher Scientific Inc., Waltham, MA). Chromatography separations were obtained on a BioBasic C18 column (180 μm i.d. × 150 mm length, 5 μm particle size), using a linear gradient from 5 to 80% solvent B [solvent A, 0.1% (v/v) formic acid; solvent B, ACN containing 0.1% (v/v) formic acid] with a flow of 2.5 μL/min. ESI was performed in positive ionization mode with spray voltage and capillary temperature set at 3 kV and at 220 °C, respectively. Data were collected in the full-scan and data-dependent MS/MS mode with collision energy of 35% and a dynamic exclusion window of 3 min.

Spectra were searched by TurboSEQUEST incorporated in Bioworks-Browser 3.2 software (ThermoFisher Scientific Inc.) against the subset of *Lolium* EST sequences database (13919 entries) and against the protein NCBI-nr database (5947209 entries), both downloaded from the National Center for Biotechnology Information (http://www.ncbi.nlm.nih.gov/). The searches were carried out by assuming parent ion and fragment ion mass tolerances of ±2 and ±1 Da, respectively, two possible missed cleavages per peptide, fixed carboxyamidomethylation of cysteine, and variable methionine oxidation. Identified peptides [Xcorr ≥1.5 (+1 charge state), ≥ 2.0 (+2 charge state), ≥ 2.5 (≥+3 charge state), peptide probability < 1 × 10^{-3}, ΔCn ≥ 0.1 and Sf ≥ 0.70] were used in the following protein similarity search performed by alignment analyses against the NCBI database using the FASTS algorithm (*33*). To validate peptide assignments, spectra were also independently searched against two created sequence-reversed databases (rev_EST and rev_NCBI-nr). This approach did not identify any hits that passed the described set of filtering criteria. Theoretical molecular mass and p*I* of the characterized proteins were calculated by processing sequence entries by ExPASy-compute pI/MW tool (http://expasy.org/tools/pi_tool.html).

RESULTS

Effect of the Chemicals on TPI Activity in Shoots of Italian Ryegrass. As an initial test, the TPI activity of protein extracts of shoots of Italian ryegrass was determined; the ryegrass was collected at 48 h after treatments performed once with each herbicide (**Table 1**). The treatments with atrazine and fluorodifen caused a significant variation in TPI activity, in comparison to untreated controls. In particular, decreases of 26.5 and 35.9%, respectively, for atrazine and fluorodifen were ascertained. The treatments with fenoxaprop-ethyl, metolachlor, and the safener fenchlorazol-ethyl did not cause significant changes in TPI activity in comparison with untreated controls.

Effect of GSSG on TPI Activity. Figure 1 shows the recovered percentage of TPI activity at 1, 3, 5, and 7 h, after starting incubation with GSSG. At the two highest concentrations of 20.4
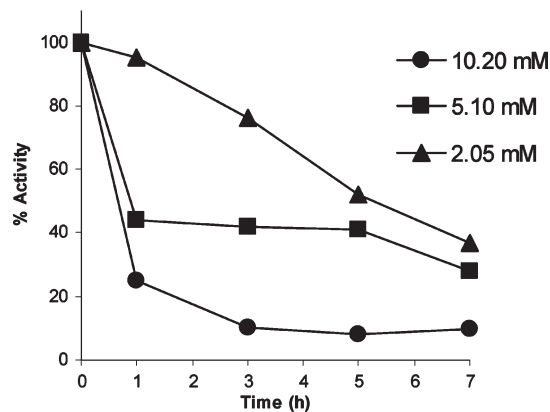

Figure 1. Extracts of shoots of Italian ryegrass were incubated at 35 °C with different concentrations of GSSG over a period of 7 h; therefore, the figure gives the percentage of TPI activity recovered compared to the controls (100% of activity), which were incubated under the same conditions without GSSG. The enzyme activity was monitored at 1, 3, 5, and 7 h after the start of incubation.

and 40.8 mM an immediate and total inactivation of TPI was observed; therefore, they are not shown in the figure. The three lower GSSG concentrations brought about significant decreases in enzyme activity; in fact, already at 1 h after the start of incubation, losses of 5, 56, and 75% of TPI activity were ascertained for GSSG concentrations of 2.05, 5.10, and 10.20 mM, respectively; these losses were continuous, and at 7 h after the start of incubation, they reached values of 63, 72, and 90% in response to GSSG concentrations of 2.05, 5.10, and 10.20 mM, respectively.

Purification of TPI Extracted from Shoots of Italian Ryegrass. Figure 2 shows a representative 2D gel of the desalted proteins, obtained by performing the IEF over a pH range from 4 to 7. Because of the large number of other proteins present (observed in the smearing), it was necessary to perform chromatographic purifications. Therefore, the desalted proteins were applied onto an anion exchanger column, and the chromatography was performed by applying an increasing gradient of NaCl. Each fraction was assayed to determine TPI activity, which eluted at increasing ionic strengths between fractions 14 and 19. **Figure 3** illustrates the profile of this chromatography, and the blue line indicates the fractions with TPI activity; for a visual evaluation of the chromatography performance, a 1D gel of three representative fractions (15−17) showing TPI activity is also given (right side of the figure). From the gel it appears that the fractions possess a large amount of polypeptides in the 25−30 kDa range, which is typical of TPI; therefore, the fractions ranging from 14 to 19 were pooled and subjected to 2D electrophoresis. **Figure 4A** shows the gel obtained: despite a decrease in the total number of spots compared to the gel of **Figure 2**, there was still a large number of spots. Therefore, the above collected fractions were rechromatographed at a flow rate of 1 mL min^{-1}, collecting fractions of 1 mL and analyzing that having the highest specific activity. **Figure 4B** shows the 2D gel of the fraction, resolved by this second chromatography, with the highest specific activity. It is evident how in this fraction the number of spots with molecular masses in the typical range of TPIs is predominant, whereas many interfering spots disappeared. The spots of interest were then excised from this gel and submitted to LC-ESI-MS/MS analyses.

Table 2 gives specific TPI activity, total TPI activity, and yield for the chromatographic steps performed. In particular, taking as 100% the protein amount and activity of desalted protein, the first chromatography gave a 1.64-fold increase of specific activity

Article

J. Agric. Food Chem., Vol. 57, No. 17, 2009 **7927**

of 14−19 collected fractions, with a recovery of 93.9% of activity. The second chromatography, performed at a flow rate of 1 mL min^{-1}, made it possible to isolate the fraction with the highest specific activity of 133.0 nmol s^{-1} mg^{-1} of protein, with a purification fold of 13.6 (**Figure 4B**).

Protein Identification. The spots having molecular masses ranging between 20 and 30 kDa, as depicted in **Figure 4**, were subjected to LC-ESI-MS/MS analysis. Because of the paucity of sequenced proteins of Italian ryegrass in the databases, the spots were identified by obtaining peptide sequences (e.g., using an EST database) and then searching similarity to homologous proteins in other species. As shown in **Table 3**, these analyses made it possible to characterize 8 spots among the 10 analyzed. Most of these spots were identified as TPIs (spots 3, 5, 6, and 12). In particular, spots 3 and 6 showed similarity with the sequence of a cTPI of *Hordeum vulgare* (accession no. P34937) and spot 12 with one of *Zea mays* (accession no. P12863). Moreover, spot 5 was assigned to a pTPI in *Secale cereale* (accession no. P46225). The predicted molecular mass of this protein is 31.6 kDa, whereas the electrophoretic analyses gave a molecular mass of 28.0 kDa. Spots 8 and 23 showed similarity with ribose-5-phosphate isomerase precursor in *Oryza sativa* (accession no. NP_001059023);
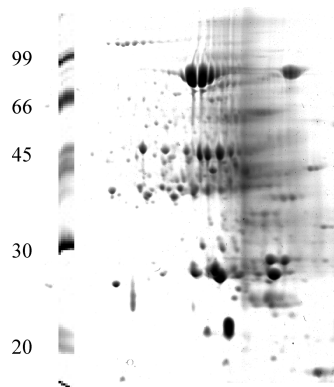
spots 29 and 30 were assigned to a sequence of copper/zinc superoxide dismutase in *Arabidopsis thaliana* (accession no. NP_565666). Finally, it was not possible to identify spots 9 and 11, probably because of the lack of related genetic information.

Figure 5 shows the identified peptides matching the respective proteins; the arrows indicate some key amino acids of TPIs present in these peptides. With regard to spot 3, Cys-67, Cys-127, Glu-166, and Gly in positions 172 and 174 were found; for spot 6, Cys-67 and Cys-127 were identified, whereas for spot 12 a Cys in position 127 was found. With regard to spot 5, in the examination of the pTPI the transit peptide was not considered, and then a Cys in position 126 was determined.

DISCUSSION

The data in **Table 1** show a decrease of TPI activity following treatments with atrazine and fluorodifen; among the five chemicals investigated, these two herbicides are known to interfere with the photosynthesis. In fact, atrazine disturbs the photosynthetic electron transfer in photosystem II, causing an altered redox status of the cell with production of ROS (*34*, *35*). Fluorodifen is a diphenyl ether herbicide, which has an inhibiting effect on protoporphyrinogen IX oxidase (Protox), a key enzyme for the biosynthesis of heme and chlorophyll (*36*). This interference causes a plasmalemma accumulation of protoporphyrinogen IX, which is a photodynamic pigment oxidized by other nonenzymatic reactions to protoporphyrin IX that brings about a rapid formation of activated oxygen and then of ROS (*37*, *38*). Instead, the other two herbicides have different target sites: metolachlor is a chloroacetanilide with multisite action, so it is able to interfere in lipid, protein, and gibberellic acid synthesis, cell division, mineral uptake, and cell permeability (*39*, *40*), whereas fenoxaprop-ethyl is an aryloxyphenoxy-propionate herbicide, which acts by inhibiting the acetyl-CoA carboxylase (*41*, *42*). Fenchlorazol-ethyl is a nontoxic herbicide safener that acts by increasing the expression of the detoxifying enzymes such as glutathione *S*-transferases (*43*). It should be pointed out that it is well-known that atrazine and fluorodifen determine an altered redox status of the cells (*34*−*36*, *38*); in addition, other experiments, performed on shoots of Italian ryegrass, showed a significant increase in antioxidant and glutathione-related enzymes in response to the two herbicides (data not shown).

This study shows that atrazine and fluorodifen caused a significant inhibition of TPI activity. To better understand the

Figure 2. 2D gel of protein fraction of Italian ryegrass shoots. Crude protein extracts of shoots of Italian ryegrass were precipitated with ammonium sulfate and then desalted by means of PD-10 columns. The desalted proteins were precipitated for 24 h at −20 °C with TCA (20% in acetone) to remove interfering substances. Shown at the left side of the figure are molecular mass markers.
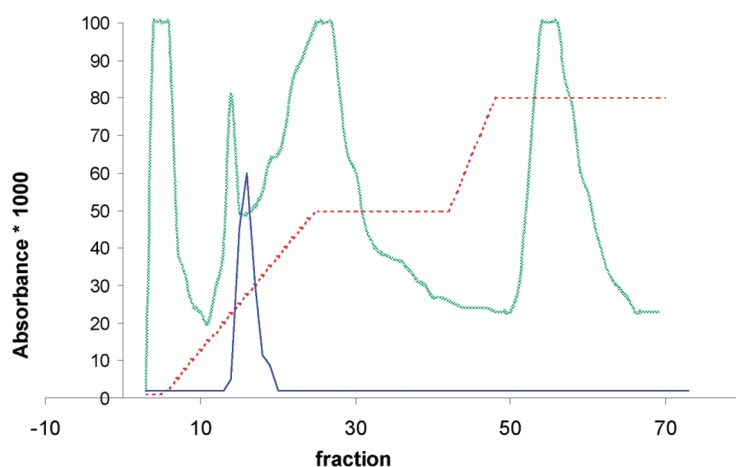
Figure 3. Desalted proteins were applied onto an anionic exchanger column, at a flow rate of 4 mL min^{-1}, collecting fractions of 4 mL, and the TPIs were eluted at increasing ionic strength: the blue line indicates the fractions where TPI activity was found, whereas the red line represents the gradient of NaCl applied, ranging from 0.0 to 0.5 M; finally, the green line indicates the profile of eluting proteins monitored at 280 nm. The right side of the figure shows a representative 1D gel: lane 1, molecular mass markers; lanes 2, 3, and 4, fractions 15, 16, and 17, respectively.

nature of this inhibition, the sensitivity of TPI to oxidative status was ascertained by incubating the enzymatic extract of untreated samples with GSSG, because it is known to be produced by ROS-stressed cells (*19*, *20*). At high concentrations, GSSG was a strong inhibitor of TPI, and it was very effective also at lower concentrations in a dose−time-dependent manner (**Figure 1**). The concentration of GSSG is increasing in conditions of ROS

Figure 4. (**A**) 2D gel of proteins charged on the column (fractions 14−19 of the first chromatography); the above fractions were rechromatographed at a flow rate of 1 mL min⁻¹, collecting fractions of 1 mL.(**B**) Gel of the fraction with the highest specific TPI activity, purified by the second chromatography. Shown at the bottom of the figure is an enlargment of gel **B**, indicating the spots subjected to LC-ESI-MS/MS.

formation, supporting the hypothesis that the two photosynthetic interfering herbicides, by causing accumulation of ROS, also increased GSSG concentration. Consequently, the cells may respond by forming the protective adduct GS−protein, which resulted in a loss of TPI activity. Some reports document that TPIs can be regulated by S-glutathionylation, through the formation of a mixed disulfide between SH residues of the protein and glutathione oxidized GSSG (*21*, *22*, *44*). The S-glutathionylation is an antioxidant device that reduces the impact of oxidants on proteins, and at the same time it is also a regulatory system for many enzyme activities (*20*, *45*−*47*).

To obtain information on protein sequences and to individuate cysteine residues probably involved in the S-glutathionylation, the TPIs were isolated and purified by a FPLC and then subjected to two-dimensional SDS-PAGE and mass spectrometry analyses. The chromatography was performed in two steps by using an anion exchanger column, which made it possible to resolve TPIs from other proteins. The 2D gel of purified fraction (**Figure 4B**) showed spots in the typical TPI mass range of 25−30 kDa.

The mass spectrometry permitted the characterization of eight proteins (**Table 3**). In particular, four spots were identified as TPIs, two spots were identified as ribose-5-phosphate isomerases, and two spots were assigned to a copper/zinc superoxide dismutase. With regard to spot 5, the identified peptides matched a precursor of a chloroplastic TPI with a hypothetical mass of 31.6 kDa. On the other hand, the molecular mass of this protein determined by electrophoresis was 28.0 kDa; in addition, among the peptides, no portion of the transit peptide (represented in green in **Figure 5**) was found. These data suggest that spot 5 is a proper mature pTPI.

Figure 5 gives the sequence and accession number of the homologous TPIs assigned by alignment analyses of the identified peptides (blue color) from Italian ryegrass spots. A high degree of analogy is evident, which is in strong accordance with the same catalytic role of these enzymes (*1*−*3*). According to the current model, His-96 and Asn-10 should be involved in stabilizing and polarizing the substrate by forming hydrogen bonds; Glu-166 serves to generate an intermediate of reaction for the final enolization, and Lys-12 should be involved in binding of substrate and catalysis (*1*, *3*, *48*). The three amino acid residues, Cys-13, -67, and -127, are considered to participate in regulation of TPI by
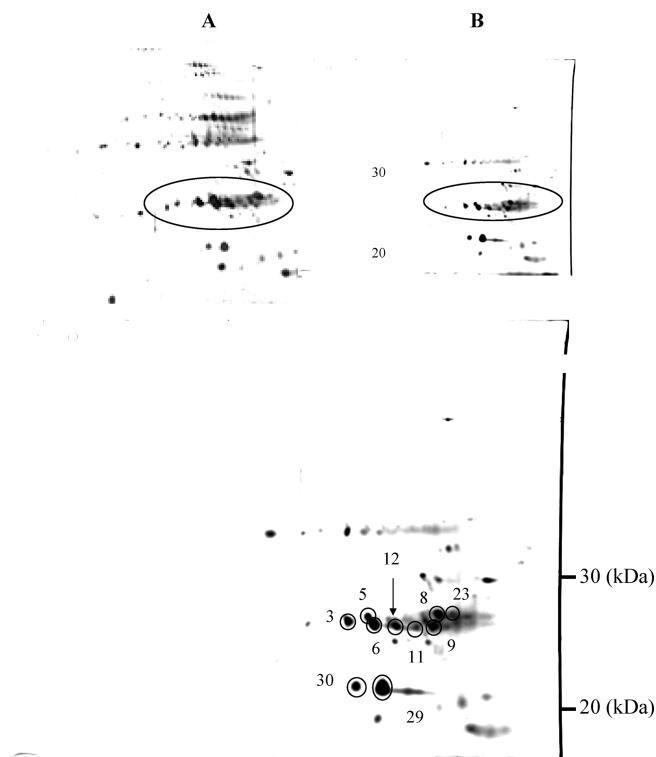
Table 2. Specific TPI Activity, Total TPI Activity, and Yield for All of the Chromatographic Steps Performed To Purify TPIs[a]

	specific activity (nmol s⁻¹ mg⁻¹ of protein)	total activity (nmol s⁻¹)	yield (%)
desalted proteins (**Figure** [2])	9.8	188.65	100.0
fractions 14−19 of the first chromatography (**Figure** [4]**A**)	16.1	177.10	93.9
fraction with the highest TPI specific activity (second chromatography, **Figure** [4]**B**)	133.0	9.31	4.9

[a] The data refer to **Figures 2**−**4**. The experiment was run in triplicate, and the table gives the most representative chromatographic result.

Table 3. Spots Identified by LC-ESI-MS/MS and Bioinformatics Analyses

spot	accession no.	species	protein description	no. of peptides[a]	M_r[b]pI[b]	M_r[c]pI[c]	cov[d] (%)
3	P34937	*Hordeum vulgare*	triosephosphate isomerase, cytosolic	8	27.0/5.7	26.7/5.4	40.7
5	P46225	*Secale cereale*	triosephosphate isomerase, chloroplast precursor	6	28.0/5.5	31.6/6.0	20.1
						27.3/5.0[e]	23.5[e]
6	P34937	*Hordeum vulgare*	triosephosphate isomerase, cytosolic	6	27.0/5.4	26.7/5.4	28.5
8	NP_001059023	*Oryza sativa*	ribose-5-phosphate isomerase precursor[f]	4	29.0/5.0	29.2/5.5	17.1
12	P12863	*Zea mays*	triosephosphate isomerase, cytosolic	6	27.0/5.2	27.0/5.5	28.1
23	NP_001059023	*Oryza sativa*	ribose-5-phosphate isomerase precursor[f]	2	29.0/5.1	29.2/5.5	6.4
29	NP_565666	*Arabidopsis thaliana*	copper/zinc superoxide dismutase 2	2	22.0/5.4	22.2/6.5	12.5
30	NP_565666	*Arabidopsis thaliana*	copper/zinc superoxide dismutase 2	2	22.0/5.6	22.2/6.5	12.5

[a] Number of unique identified peptides. [b] Experimental molecular mass (kDa) or isoelectric point. [c] Theoretical molecular mass (kDa) or isoelectric point. [d] Amino acid coverage. [e] Values referred to the mature form of the protein. [f] Information obtained from the features indicated by the authors. Statistical information is given in the Supporting Information.

Spot 3   cytosolic TPI (P34937)

```
         10                                    50                    ↓                              100
MGRKFFVGGN WKCNGTVEQV EAIVQTLNAG QIVSPDVVEV VVSPPYVFLP IVKAKLRPEI QVAAQNCWVK KGGAFTGEVS AEMLANLGVP WVILGHSERR
                                            150              ↓          ↓ ↓                         200
SLLGESSEFV GEKVAYALAQ GLKVIACVGE TLEQREAGST MEVVAEQTKA IAGKIKDWSN GVVAYEPVWA IGTGKVATPA QAQEVHANLR DWLKTNVSPE
         250
VAESTRIIYG GSVTGASCKE LAAQADVDGF LVGGASLKPE FIDIINAAAV KSA
```

Spot 6   cytosolic TPI (P34937)

```
         10                                    50                    ↓                              100
MGRKFFVGGN WKCNGTVEQV EAIVQTLNAG QIVSPDVVEV VVSPPYVFLP IVKAKLRPEI QVAAQNCWVK KGGAFTGEVS AEMLANLGVP WVILGHSERR
                    ↓                       150                                                     200
SLLGESSEFV GEKVAYALAQ GLKVIACVGE TLEQREAGST MEVVAEQTKA IAGKIKDWSN GVVAYEPVWA IGTGKVATPA QAQEVHANLR DWLKTNVSPE
         250
VAESTRIIYG GSVTGASCKE LAAQADVDGF LVGGASLKPE FIDIINAAAV KSA
```

Spot 12   cytosolic TPI (P12863)

```
         10                                    50                                                  100
MGRKFFVGGN WKCNGTTDQV EKIVKTLNEG QVPPSDVVEV VVSPPYVFLP VVKSQLRQEF HVAAQNCWVK KGGAFTGEVS AEMLVNLGVP WVILGHSERR
                                            150                      ↓                              200
ALLGESNEFV GDKVAYALSQ GLKVIACVGE TLEQREAGST MDVVAAQTKA IAEKIKDWSN VVVAYEPVWA IGTGKVATPA QAQEVHASLR DWLKTNASPE
         250
VAESTRIIYG GSVTAANCKE LAAQPDVDGF LVGGASLKPE FIDIINAATV KSA
```

Spot 5   chloroplast precursor TPI (P46225)

```
         10                                    50                                                  100
MAARRPSPPP ASPPPPRPRS TTTTRTTSSA SAAPAAAQRL VAMAGSGKFF VGGNWKCNGT KESISKLVSD LNAATLESDV DVVVAPPFIY IDQVKSSLTD
                                            150                      ↓                              200
RIEVSAQNTW IGKGGAFTGE ISAEQLVDIG CQWVILGHSE RRHVIGEDDE FIGKKAAYAL SQNLKVMACI GELLEEREAG KTFDVCFKQM KAFADNITDW
                                            250
TNVVIAYEPV WAIGTGKVAS PEQAQEVHAA VRDWLKTNVS ADVASTVRII YGGSVNAANC AELAKKEDID GFLVGGASLK GPDFATICNS VTSKKVTA
```

Figure 5. Peptides (blue) matching the homologous protein sequence (accession no. in parentheses). The green sequence is relative to the transit peptide for transport of pTPI in chloroplast.

S-glutathionylation, although Cys-67 is not present in pTPI (*1, 2, 49*). Glu-167, or in position 165 as reported by other authors, causes a partial enolization of substrate by interaction with the proton of C1 of DHAP or, in the reversed reaction, by interaction with the proton of C2 of GAP, whetrsd Gly-173, Ser-213, and Gly 234 serve as phosphate moiety (*2, 3, 48*).

In regard to the TPIs characterized in this research (**Figure 5**), some of the above key amino acids are present in the identified peptide. In particular, with regard to cysteine residues that are involved in the S-glutathionylation of TPIs, Cys-67, Cys-127, and Cys-126 were found. The pTPI does not show in position 67 (without considering the transit peptide) any cysteine residues; this is consistent with that already observed for other pTPIs (*2*). Therefore, the mass spectrometry analyses made it possible to individuate peptides having some cysteine residues that could be subjected to S-glutathionylation by reacting with GSSG via a thiol−sulfide exchange. In fact, the key residues Cys-67 and -127 found in TPIs of Italian ryegrass can be involved in the formation of the protective and regulating mixed disulfide bonds GS−protein.

In conclusion, the sensitivity of TPIs to stressing agents, such as herbicides interfering with photosynthesis, and their dose−time-dependent response to GSSG have been shown. FPLC permitted the isolation and purification of enzyme extracts; two-dimensional electrophoresis and mass spectrometry made it possible to characterize four TPIs, pointing out the presence of cysteine residues in key positions for the regulation of enzyme activity by S-glutathionylation.

Supporting Information Available: Sequence of all peptides identified by MS/MS fragmentation and associated statistical information. This material is available free of charge via the Internet at http://pubs.acs.org.

LITERATURE CITED

(1) Henze, K.; Schnarrenberger, C.; Kellermann, J.; Martin, W. Chloroplast and cytosolic triosephosphate isomerases from spinach: purification, microsequencing and cDNA cloning of the chloroplast enzyme. *Plant Mol. Biol.* **1994**, *26*, 1961–1973.

(2) Dorion, S.; Parveen, J. J.; Jeukens, J.; Matton, D. P.; Rivoal, J. Cloning and characterization of a cytosolic isoform of triosephosphate isomerase developmentally regulated in potato leaves. *Plant Sci.* **2005**, *168*, 235–243.

(3) Komives, E. A.; Chang, L. C.; Lolis, E.; Tilton, R. F.; Petsko, G. A.; Knowles, J. R. Electrophilic catalysis in triosephosphate isomerase: the role of histidine − 95. *Biochemistry* **1991**, *30*, 3011–3019.

(4) Tomlinson, J. D.; Turner, J. F. Pea seeds triose phosphate isomerase. *Phytochemistry* **1979**, *18*, 1959–1962.

(5) Tang, G. L.; Wang, Y. F.; Bao, J. S.; Chen, H. B. Overexpression in Escherichia coli and characterization of the chloroplast triosephosphate isomerase from spinach. *Prot. Exp. Purif.* **1999**, *16*, 432–439.

(6) Pichersky, E.; Gotlieb, L. D. Plant triose phosphate isomerase isozymes. Purification, immunological and structural characterization, and partial amino acid sequences. *Plant Physiol.* **2000**, *122*, 767–774.

(7) Schnarrenberger, C.; Jacobshagen, S.; Müller, B.; Krüger, I. Evolution of isozymes of sugar phosphate metabolism in green algae. In *Isozymes: Structure, Function and Use in Biology and Medecine*; Wiley-Liss: New York, 1990; pp 743−764.

(8) Miernyk, J. A. Glycolysis, the oxidative pentose phosphate pathway and anaerobic respiration. In *Plant Physiology, Biochemistry and Molecular Biology*; Dennis, D. T., Turpin, D. H., Eds.; Longman Scientific and Technical: Harlow, U.K., 1990; pp 77−100.

(9) Xu, Y.; Hall, T. C. Cytosolic triosephosphate isomerase is a single gene in rice. *Plant Physiol.* **1993**, *101*, 683–687.

(10) Marchionni, M.; Gilbert, W. The triosephosphate isomerase gene from maize: introns antenate the plant-terminal divergence. *Cell* **1986**, *46*, 133–141.

(11) Deepika, M.; Grover, A. Transcript levels of genes encoding various glycolytic and fermentation enzymes change in response to abiotic stress. *Plant Sci.* **1999**, *146*, 41–51.

(12) Umeda, M.; Hara, C.; Matsubayashi, Y.; Li, Hh.; Liu, Q.; Tadokoro, F.; Aotsuka, S.; Uchimiya, H. Expressed sequence tags from cultured-cells of rice (*Oryza-sativa*) under stressed conditions— analysis of transcripts of genes engaged in atp-generating pathways. *Plant Mol. Biol.* **1994**, *25*, 469–478.

Del Buono et al.

(13) Riccardi, F.; Gazeau, P.; De Vienne, D.; Zivy, M. Protein change in response to progressive water deficit in maize. *Plant Physiol.* **1998**, *117*, 1253–1263.

(14) Subramanian, B.; Bansal, V. K.; Kav, N. N. V. Protome-level of *Brassica carinata*-dervided resistance to *Leptosphaeria maculans. J. Agric. Food Chem.* **2005**, *53*, 313–324.

(15) Zhang, Y.; Yuksel, U.; Gracy, R. W. Terminal marking of avian triosephosphate isomerases by deamidation and oxidation. *Arch. Biochem. Biophys.* **1995**, *317*, 112–120.

(16) Baxter, C. J.; Redestig, H.; Schauer, N.; Repsilber, D.; Patil, K. R.; Nielsen, J.; Selbig, J.; Liu, J.; Fernie, A. R.; Sweetlove, L. The metabolic response of heterotrophic *Arabidopsis* cells to oxidative stress. *Plant Physiol.* **2007**, *143*, 312–325.

(17) Mittler, R. Oxidative strees, antioxidants and stress tolerance. *Trends Plant Sci.* **2002**, *7*, 405–410.

(18) Mittler, R. Abiotic stress, the field environment and stress combination. *Trends Plant Sci.* **2006**, *11*, 15–19.

(19) Ball, L.; Accotto, G. P.; Bechtold, U.; Creissen, G.; Funck, D.; Jimenez, A.; Kular, B.; Leyland, N.; Mejia-Carranza, J.; Reynolds, H.; Karpinski, S.; Mullineaux, P. M. Evidence for a direct link between glutathione biosynthesis and stress defence gene expression in *Arabidopsis. Plant Cell* **2004**, *16*, 2448–2462.

(20) Michelet, L.; Zaffagnini, M.; Marchand, C.; Collin, V.; Decottignies, P.; Tsan, P.; Lancelin, J. M.; Trost, P.; Miginiac-Maslow, M.; Noctor, G.; Lemaire, S. D. Glutathionylation of chloroplast thioredoxin f is a redox signaling mechanism in plants. *Proc. Natl. Acad. Sci. U.S.A.* **2005**, *102*, 16478–16483.

(21) Hwang, C.; Sinskey, A. J.; Lodish, H. F. Oxidized redox state of glutathione in the endoplasmic-reticulum. *Science* **1992**, *257*, 1496–1502.

(22) Fratelli, M.; Demol, H.; Puype, M.; Casagrande, S.; Eberini, I.; Salmona, M.; Bonetto, V.; Mengozzi, M.; Duffieux, F.; Miclet, E.; Bachi, A.; Vandekerckhove, J.; Gianazza, E.; Ghezzi, P. Identification by redox proteomics of glutathionylated proteins in oxidatively stressed human T lymphocytes. *Proc. Natl. Acad. Sci. U.S.A.* **2002**, *99*, 3505–3510.

(23) Davies, J.; Caseley, J. C. Herbicide safeners: a review. *Pestic. Sci.* **1999**, *55*, 1043–1058.

(24) Abu-Qare, A. W.; Duncan, H. J. Herbicide safeners: uses, limitations, metabolism, and mechanisms of action. *Chemosphere* **2002**, *48*, 965–974.

(25) Hatzios, K. K.; Burgos, N. Metabolism-based herbicide resistance: regulation by safeners. *Weed Sci.* **2004**, *52*, 454–467.

(26) Peleg, I.; Zer, H.; Chevion, M. Paraquat toxicity in *Pisum-sativum* — effects on soluble and membrane-bound proteins. *Physiol. Plant.* **1992**, *86*, 131–135.

(27) Growald, J. W.; Eberlein, C. V.; Betts, K. J.; Baerg, R. J.; Ehlike, N. J.; Wyse, D. L. Mechanism of diclop resistance in an Italian ryegrass (*Lolium multiflorum*) byotipe. *Pestic. Biochem. Physiol.* **1992**, *44*, 126–139.

(28) De Prado, R.; Gonzàlez-Gutiérrez, J.; Menéndez, J.; Gasquez, J.; Gronwald, J. W. Resistance to acetyl CoA carboxylase-inhibiting herbicides in *Lolium multiflorum. Weed Sci.* **2000**, *48*, 311–318.

(29) Bradford, M. A rapid and sensitive method for the quantitation of microgram quantities of protein utilizing the principle of protein–dye binding. *Anal. Biochem.* **1976**, *72*, 248–254.

(30) Laemmli, U. K. Cleavage of structural proteins during the assembly of the head of bacteriofage T4. *Nature* **1970**, *227*, 680–685.

(31) O'Farrel, P. H. High-resolution two-dimensional electrophoresis of proteins. *J. Biol. Chem.* **1975**, *250*, 4007–4021.

(32) Magni, C.; Scarafoni, A.; Herndl, A.; Sessa, F.; Prinsi, B.; Espen, L.; Duranti, M. Combined 2D electrophoretic approaches for the study of white lupin mature seed storage proteome. *Phytochemistry* **2007**, *68*, 997–1007.

(33) Mackey, A. J.; Haystead, T. A. J.; Pearson, W. R. Getting more from less: algorithms for rapid protein identification with multiple short peptide sequences. *Mol. Cell Proteomics* **2002**, *1*, 139–147.

(34) El-Shintinawy, F.; El-Shourbagy, M. N. Recovery of photosystem 2 and membrane lipid composition in triazine-treated soybean seedlings by vitamins. *Biol. Plant.* **1997**, *39*, 633–636.

(35) Ivanov, S. V.; Alexieva, V. S.; Karanov, E. N. Cumulative effect of low and high atrazine concentrations on *Arabidopsis thaliana* plants. *Russ. J. Plant Physiol.* **2005**, *52*, 213–219.

(36) Retzlaff, K.; Boger, P. An endoplasmatic plant enzyme has protoporphyrinogen IX oxidase activity. *Pestic. Biochem. Physiol.* **1996**, *54*, 105–114.

(37) Camadro, J. M.; Matringe, M.; Brouillet, N.; Thome, F.; Labbe, P. Characterization of plant and yeast protoporphyrinogen oxidase — molecular target of diphenyl ether type herbicides. In *Porphyric Pesticides — Chemistry, Toxicology and Pharmaceutical Applications. ACS Symp. Ser.* **1994**, *No. 559*, 81–90.

(38) Jung, H. I.; Kuk, Y. I.; Back, K.; Burgos, N. R. Resistance pattern and antioxidant enzyme profiles of protoporphyrinogen oxidase (PROTOX) inhibitor-resistant transgenic rice. *Pestic. Biochem. Physiol.* **2008**, *91*, 53–65.

(39) Fuerst, E. P. Understanding the mode of action of chloroacetamide and thiocarbamates. *Weed Technol.* **1987**, *1*, 270.

(40) Wu, J.; Hwang, I. T.; Hatzios, K. K. Effects of chloroacetanilide herbicides on membrane fatty acid desaturation and lipid composition in rice, maize and sorghum. *Pestic. Biochem. Physiol.* **2000**, *66*, 161–169.

(41) Hall, L. M.; Moss, S. R.; Powles, S. B. Mechanisms of resistance to aryloxyphenoxypropionate herbicides in two resistant biotypes of *Alopecurus myosuroides* (blackgrass): herbicide metabolism as a croosresistance mechanism. *Pestic. Biochem. Physiol.* **1997**, *57*, 87–98.

(42) Bakkali, Y.; Ruiz-Santaella, J. P.; Osuna, M. D.; Wagner, J.; Fischer, A. J.; De Prado, R. Late watergrass (*Echinochloa phyllopogon*): mechanisms involved in the resistance to fenoxaprop-*p*-ethyl. *J. Agric. Food Chem.* **2007**, *55*, 4052–4058.

(43) Cummins, I.; Cole, D. J.; Edwards, R. Purification of multiple glutathione transferases involved in herbicide detoxification from wheat (*Triticum aestivum* L.) treated with the safener fenchlorazole-ethyl. *Pestic. Biochem. Physiol.* **1997**, *59*, 35–49.

(44) Dixon, D. P.; Skipsey, M.; Grundy, N. M.; Edwards, R. Stress-induced protein S-glutathionylation in *Arabidopsis. Plant Physiol.* **2005**, *138*, 2233–2244.

(45) Chrestensen, C. A.; Starke, D. W.; Mieyal, J. J. Acute cadmium exposure inactivates thioltransferase (glutaredoxin), inhibits intracellular reduction of protein-glutathionyl-mixed disulfides, and initiates apoptosis. *J. Biol. Chem.* **2000**, *275*, 26556–26565.

(46) D'Andrea, T.; Bajak, E.; Warngard, L.; Cotgreave, I. A. Protein S-glutathionylation correlates to selective stress gene expression and cytoprotection. *Arch. Biochem. Biophys.* **2002**, *406*, 241–252.

(47) Di Stefano, A.; Frosali, S.; Leonini, A.; Ettorre, A.; Priora, R.; Di Simplicio, F. C.; Di Simplicio, P. GSH depletion, protein S-glutathionylation and mitochondrial transmembrane potential hyperpolarization are early events in initiation of cell death induced by a mixture of isothiazolinones in HL60 cells. *Biochim. Biophys. Acta Mol. Cell. Res.* **2006**, *1763*, 221–225.

(48) Stroppolo, M. E.; Falconi, M.; Caccuri, A. M.; Desideri, A. Review — superefficient enzymes. *Cell. Mol. Life Sci.* **2001**, *58*, 1451–1460.

(49) Rathinasabapathi, B.; Wu, S.; Sundaram, S.; Rivoal, J.; Srivastava, M.; Ma, L. Q. Arsenic resistance in *Pteris vittata* L.: identification of a cytosolic triosephosphate isomerase based on cDNA expression clonino in *Escherichia coli. Plant Mol. Biol.* **2006**, *62*, 845–857.